Supplemental Information

Supplemental Methods and Materials

Biological Samples and Neurochemical Analyses

Cerebrospinal fluid (CSF, 2 ml) was collected from each monkey via cisternal puncture under ketamine anesthesia (10 mg/kg, i.m.). All samples were collected between 11:30 and 14:30, and ketamine was injected within 15 min of investigators' entrance into the housing facility for capture. Due to sample contamination, data from five animals (3 MR males, 1 MR female, 1 PR female) were not analyzed. CSF was immediately aliquoted into polypropylene tubes and frozen in liquid nitrogen. Determination of CSF 5-HIAA was performed with high-performance liquid chromatography followed by electrochemical detection [previously described (1)].

Imaging Data

Magnetic resonance imaging (MRI). Structural brain images were acquired on a 3.0 Tesla Siemens Magnetom Allegra MRI (Siemens Medical Solutions, Inc., Malvern, PA). MRI and PET acquisitions were separated by at least 2 days to allow full recovery between studies. To maintain anesthesia, each MRI scan was performed under continuous i.v. infusion of 9-14 mg/kg/h Saffan or 40-60 mg/kg/h propofol. The parameters for the 3D T1 MPRAGE acquisition were: TR/TE/TI: 2500/3.49/1000 ms, 1 slab of 224 slices: 0.60 mm thickness, 0.30 mm spacing, flip angle 8°, and matrix 256 x 256. The acquisition was run at 4NEX using a Nova DR dual surface coil. The 3D slab was placed over the entire brain, centered and angled on the anterior -

posterior commissures (AC/PC) line. The same head holder and mask were used for both the PET and MRI scans.

Region-of-interest (ROI) placement. Bilateral ROIs were drawn on the T1 MRI images of each monkey with reference to a stereotaxic atlas (2). The MRI image was resliced into the same space and voxel size (1.14 mm x 1.14 mm x 2.45 mm) as the PET image and the ROI were defined on the MRI images and then used to measure the [^{18}F]FPWAY concentration in the co-registered PET images as an averaged concentration in all ROIs in the structure of interest. A single ROI represented a circle sized between 63 and 73 mm^3 or 20-24 voxels placed in the center of the structure of interest on two-three consecutive slices except the dmPFC, for which ROI was placed on a single slice only (see Figure S1). For AMY, HC and cerebellum ROIs were placed in each hemisphere, for ACC, MCC and RN a single ROI in the midline covered right- and left-sided brain regions. Total ROI volumes for each structure calculated as a sum of single ROIs were: cerebellum – 260.4 mm^3, RN – 206.0 mm^3, dmPFC - 132.0 mm^3, ACC - 203.4 mm^3, MCC – 136.7 mm^3, HC – 279.0 mm^3 and AMY – 413.0 mm^3. Since no differences were found between time activity curves for HP, AMY, dmPFC and cerebellum from right and left hemispheres, data from left- and right-sided brain areas were averaged. The above standard ROI template was copied to each monkey's MRI and the position of each ROI was adjusted, if necessary, without changes in volume.

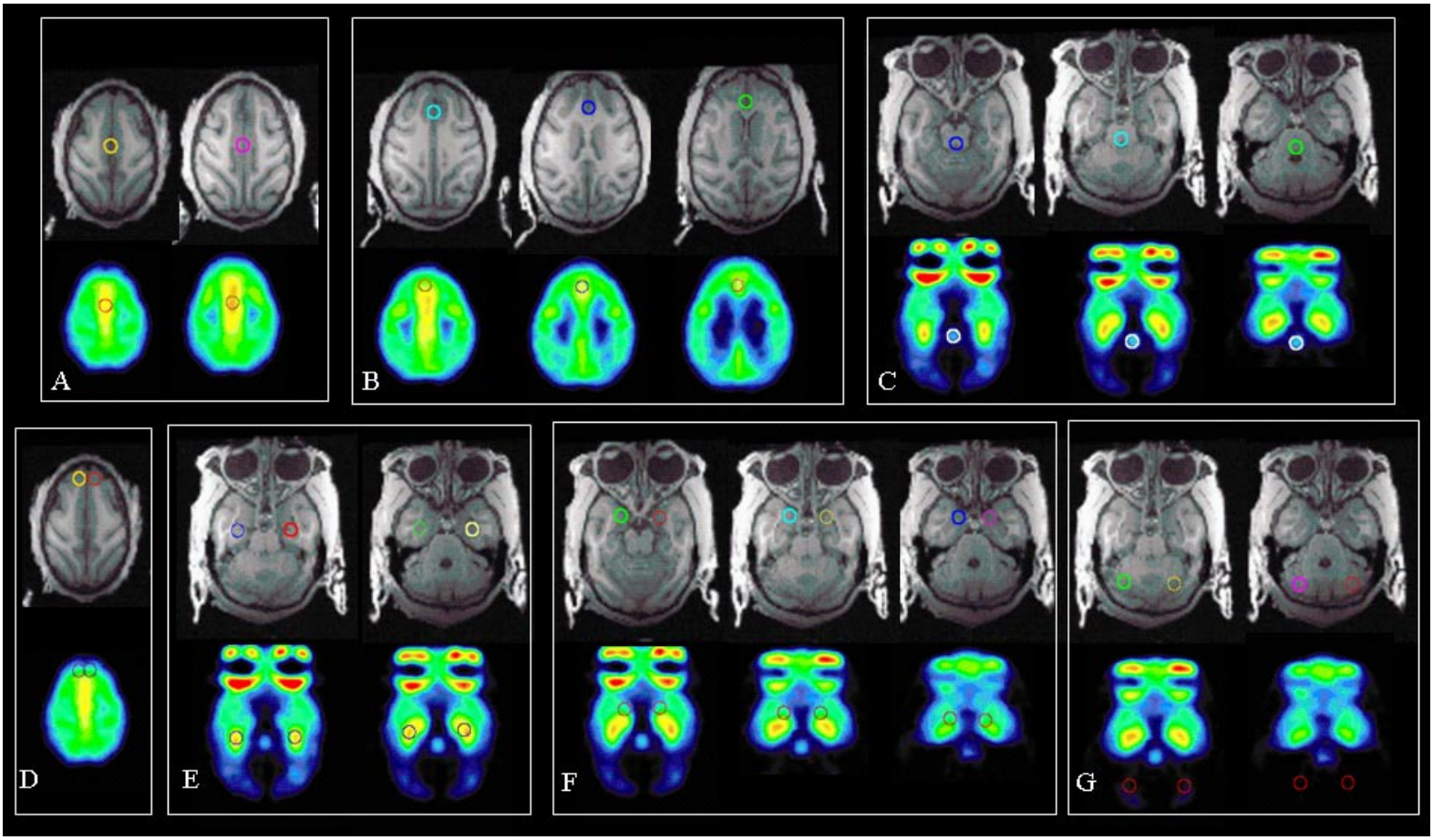

Figure S1. Co-registered MRI (upper) and PET (lower) sections through different levels of the brain showing the ROI placement in the (**A**) medial cingulate cortex (MCC), (**B**) anterior cingulate cortex (ACC), (**C**) midbrain raphe nuclei (RN), (**D**) dorsomedial prefrontal cortex (dmPFC), (**E**) hippocampus (HC), (**F**) amygdala (AMY), and (**G**) cerebellum (CB) used a reference region to measure a non-displaceable radioligant accumulation.

PET Data Analyses

Binding potential (BP) was calculated by two approaches: 1) as the ratio of specifically bound radioligand concentration to that of non-displaceable radioligand concentration in tissue ($(C_{ROI} - C_{ND})/C_{ND}$) at equilibrium ($BP_{ND} = (C_{ROI} - C_{ND})/C_{ND} = f_{ND}B_{max}/K_D^{app}$) and 2) as the ratio of specifically bound radioligand concentration to free radioligand concentration in plasma (C_p) at equilibrium ($BP_F = (C_{ROI} - C_{ND})/C_{p)} = f_pB_{max}/K_D^{app}$). Both derivations of BP are linearly

proportional to B_{max} and $1/K_{D,}$ and changes in B_{max} or $1/K_D$ should affect these two measures of BP similarly. In addition, since data in humans indicate sex difference in the cerebellar volume of distribution what might be a bias for calculating BP_{ND} (3) it was necessary to compare C_{ND}/C_p ratio as a function of sex and rearing. Nevertheless, intra- and inter-study variability of the two BP measures might be substantially different owing to several methodological factors. Thus, receptor quantification using the two methods maximized the reliability of the interpretation of the data and enhanced confidence that statistically significant differences are truly receptor-related signals and not methodological artifact. However, as a general rule, BP_{ND} shows lower error than BP_F, because any measurement errors in the arterial input function and metabolites tend to cancel out in the former measure. Since only a limited blood volume could be withdrawn from 2 years old rhesus monkeys, it is possible that assays for the non-metabolized parent compound plasma fraction may suffer from low statistical reliability.

As a region devoid of 5-HT_{1A}R (4, 5), the cerebellum provided an estimate of the sum of concentrations of free and non-specifically bound radioligand (6) (non-displaceable accumulation of radioligand). To verify that the fraction of free plus non-specifically bound radioligand did not differ between male and female or between MR and PR groups, we compared the C_{ND}/C_p ratio (V_{ND}) as a function of sex and rearing (see Supplemental Results).

Supplemental Results

Effects of Rearing Conditions and Sex on Plasma [^{18}F]FPWAY Fraction

Importantly, there were no effects of rearing ($F(1,17) = 0.02$, $p > 0.88$) or gender ($F(1,17) = 0.09$, $p > 0.76$) or rearing X gender interaction ($F(1,17) = 0.71$, $p > 0.41$) on V_{ND} values

measured in the cerebellum (females MR/PR: 2.35 ± 0.13/2.44 ± 0.18, males MR/PR: 2.42 ± 0.11/2.29 ± 0.08), indicating that the area used to assess a non-specific binding of radioligand was not affected either by gender or rearing condition. These results also favored the use of cerebellum as a reference region for BP_{ND} measurement.

Since there appears to be some 5-HT_{1A}R in the cerebellum, at least in humans (4, 7), to exclude the possibility of measuring even small levels of specific binding in the cerebellum, the ROIs were drawn on the cerebellar white matter (5).

Effects of Rearing Conditions and Sex on BP_F

As expected, analysis of BP_F values (mL/cc), calculated using the free concentration of [^{18}F]FPWAY in plasma not bound to plasma proteins, showed similar results with BP_{ND} data. MANOVA of BP_F revealed a significant main effect of rearing condition ($F(6,12) = 3.57$, $p < 0.03$), and no effect of gender ($F(6,12) = 0.54$, $p > 0.76$), or rearing X gender interaction ($F(6,12) = 1.05$, $p > 0.44$). For the dmPFC, two-way ANOVA on BP_F showed a significant rearing X gender interaction ($F(1,17) = 4.57$, $p < 0.05$), but no rearing ($F(1,17) = 2.77$, $p > 0.11$) or gender ($F(1,17) = 0.73$, $p > 0.40$) effects. Female PR monkeys showed a significant increase in BP_F in the dmPFC compared to female MR monkeys ($t(1,8) = -2.75$, $p < 0.03$; Figure S2A), but not in males in this area ($t(1,9) = 0.33$, $p > 0.74$; Figure S2B). Two-way ANOVA for BP_F of the ACC and MCC showed a tendency for a significant rearing X sex interaction ($F(1,17) = 3.86$, $p < 0.07$; $F(1,17) = 3.51$, $p < 0.08$; respectively) which can be related to the lower precision of BP_F compared to BP_{ND} due to measurement errors in the non-metabolized parent compound plasma fraction.

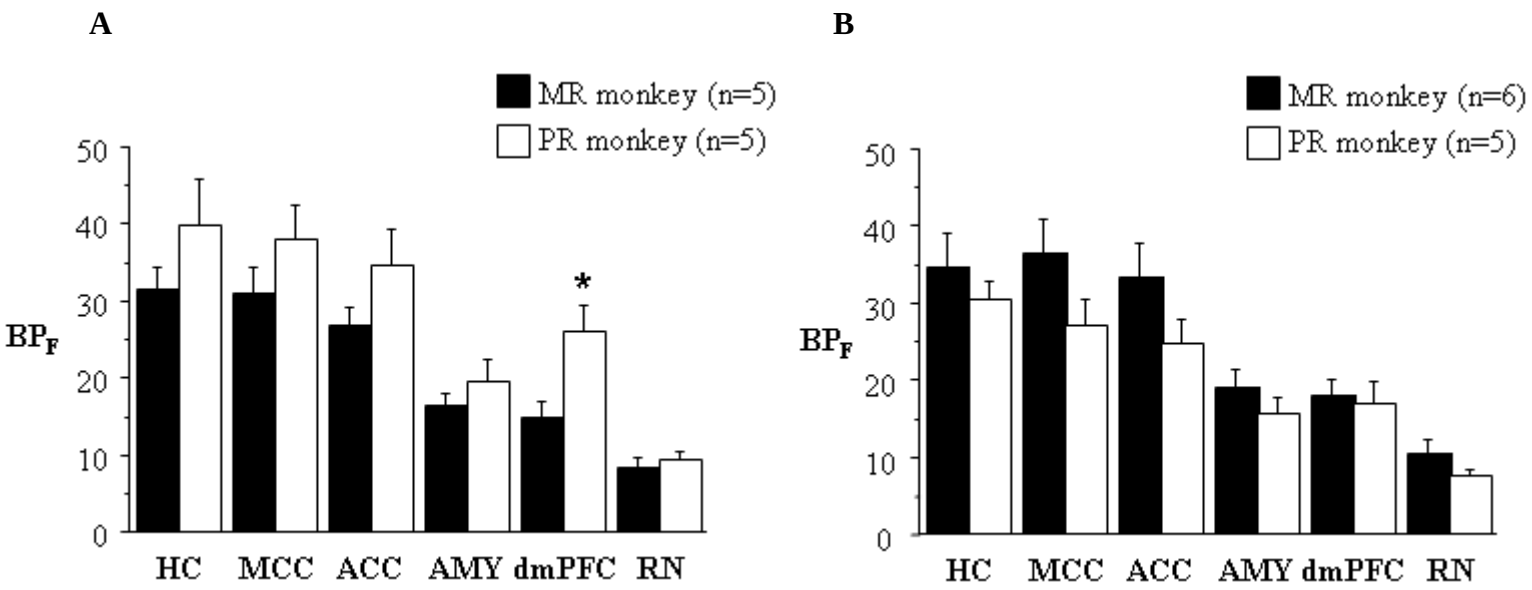

Figure S2. Effects of peer-rearing on BP_F values (mL/cc) obtained with [^{18}F]FPWAY in (**A**) female and (**B**) male monkeys. Each column represents mean $\pm$ SEM, *unpaired t-test $p < 0.03$. HC, hippocampus; MCC, medial cingulate cortex; ACC, anterior cingulate cortex; AMY, amygdala; dmPFC, dorsomedial prefrontal cortex; RN, raphe nuclei (midbrain)

Supplemental Discussion

Figure S3 illustrates how changes in B_{max} or K_D^{app} values can influence BP using results from the current study. When a decrease in K_D^{app} occurs concomitant with a smaller decrease in B_{max}, a small (10%) increase in BP is seen (Figure S3A). A small increase in B_{max} with a modest decrease in K_D^{app} induces a much greater increase in BP (>50%) (Figure S3B), leading to the largest increase in BP found in this study. In contrast, a reduction in B_{max} with a smaller decrease in K_D^{app} value results in a decline in BP (Figure S3C). However, in brain areas where similar changes in the same direction in both B_{max} and K_D^{app} occur, changes in BP are negligible (Figure S3D). As a result, even small non-statistically significant but simultaneous alterations in

B_{max} and K_D^{app} may lead to substantial changes in BP, suggesting the importance of contributions of both parameters to the measured BP value.

It should also be noted that the BP values measured during the later portion of the study (when the receptors are partially blocked by the unlabelled ligand) have higher variance (due to radioactive decay and lower contrast); such errors will affect both B_{max} and K_D^{app} estimations, with little effect on BP, which is determined primarily from the early part of the data using higher brain radioactivity concentrations.

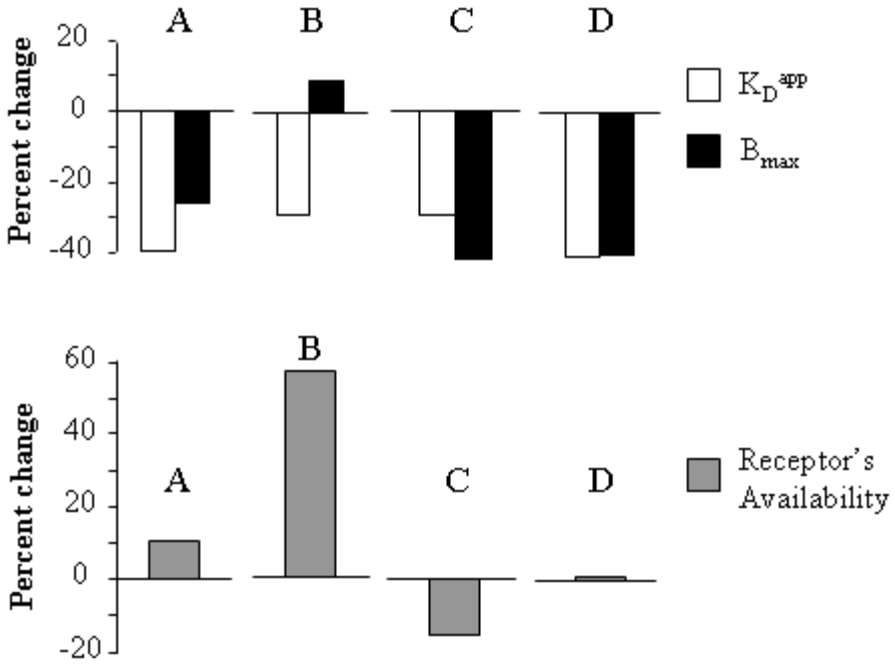

Figure S3. Interpretation of changes in receptor's availability as a function of changes in B_{max} and K_D^{app}. (**A**) Small increase in availability can result from a concomitant decrease in B_{max} and K_D^{app}. (**B**) Large increase in availability can be the consequence of a small increase in B_{max} and a relatively large decrease in K_D^{app}. (**C**) Decline in availability can occur with a reduction in B_{max} and a relatively smaller decrease in K_D^{app}. (**D**) Changes in availability are negligible when similar changes in B_{max} and K_D^{app} occur.

We found an increase in B_{max} (31%) in the dmPFC in female PR monkeys and a concomitant decrease in K_D^{app} (-23%) that lead to an overall substantial increase in BP_{ND} (56%) in this area. In contrast, in male PR monkeys, we found a decrease in B_{max} in the MCC (-43%) and the ACC (-37%) and, similar to females, a decrease in K_D^{app} (-18 and -17%) that translated in an overall decrease in 5-HT_{1A}R availability in the MCC (-18%) and in the ACC (-17%) [See Tables 2, 3 and 4 in the main article].

Additional limitation of the study. *In vitro* studies have reported high levels of 5-HT_{1A}R in the midbrain RN (7). However, due to the small size of this region and the limited spatial resolution of PET, partial volume effects likely reduced RN receptor measurement sensitivity (8). Indeed, although Giovacchini and colleagues were able to visualize the RN in adult rhesus monkeys using FPWAY, the order of BP_{ND} values in comparison with other brain areas was much lower than expected from *in vitro* data (9).

1. Shannon C, Schwandt ML, Champoux M, Shoaf SE, Suomi SJ, Linnoila M, *et al.* (2005): Maternal absence and stability of individual differences in CSF 5-HIAA concentrations in rhesus monkey infants. *Am J Psychiatry* 162: 1658-1664.
2. Saleem KS, Logothetis NK (2006): *A combined MRI and histology atlas of the rhesus monkey brain in stereotaxic coordinates*. San Diego, CA: Academic Press.
3. Parsey RV, Oquendo MA, Simpson NR, Ogden RT, Van Heertum R, Arango V, *et al.* (2002): Effects of sex, age, and aggressive traits in man on brain serotonin 5-HT1A receptor binding potential measured by PET using [C-11]WAY-100635. *Brain Res* 954: 173-182.

4. Hall H, Lundkvist C, Halldin C, Farde L, Pike VW, McCarron JA, *et al.* (1997): Autoradiographic localization of 5-HT1A receptors in the post-mortem human brain using [3H]WAY-100635 and [11C]way-100635. *Brain Res* 745: 96-108.

5. Parsey RV, Arango V, Olvet DM, Oquendo MA, Van Heertum RL, Mann JJ (2005): Regional heterogeneity of 5-HT1A receptors in human cerebellum as assessed by positron emission tomography. *J Cereb Blood Flow Metab* 25: 785-793.

6. Carson RE, Channing MA, Der MG, Herscovitch P, Eckelman WC (2002): Scatchard analysis with bolus/infusion administration of [11C]raclopride; amphetamine effects in anesthetized monkeys. In: Senda M, Kimura Y, Herscovitch P (eds). *Brain imaging using PET*. San Diego, CA: Academic Press, pp 63-96.

7. Varnas K, Halldin C, Hall H (2004): Autoradiographic distribution of serotonin transporters and receptor subtypes in human brain. *Hum Brain Mapp* 22: 246-260.

8. Stein P, Savli M, Wadsak W, Mitterhauser M, Fink M, Spindelegger C, *et al.* (2008): The serotonin-1A receptor distribution in healthy men and women measured by PET and [carbonyl-(11)C]WAY-100635. *Eur J Nucl Med Mol Imaging* 35:2159-68.

9. Giovacchini G, Lang L, Ma Y, Herscovitch P, Eckelman WC, Carson RE (2005): Differential effects of paroxetine on raphe and cortical 5-HT1A binding: a PET study in monkeys. *Neuroimage* 28: 238-248.